JACS
JOURNAL OF THE AMERICAN CHEMICAL SOCIETY
Article
pubs.acs.org/JACS

Gain-of-Function Analogues of the Pore-Forming Peptide Melittin Selected by Orthogonal High-Throughput Screening

Aram J. Krauson, Jing He, and William C Wimley*

Department of Biochemistry, SL43, Tulane University School of Medicine, New Orleans, Louisiana 70112, United States

Supporting Information

ABSTRACT: We recently developed an orthogonal, high-throughput assay to identify peptides that self-assemble into potent, equilibrium pores in synthetic lipid bilayers. Here, we use this assay as a high-throughput screen to select highly potent pore-forming peptides from a 7776-member rational combinatorial peptide library based on the sequence of the natural pore-forming peptide toxin melittin. In the library we varied ten critical residues in the melittin sequence, chosen to test specific structural hypotheses about the mechanism of pore formation. Using the new high-throughput assay, we screened the library for gain-of-function sequences at a peptide to lipid ratio of 1:1000 where native melittin is not active. More than 99% of the library sequences were also inactive under these conditions. A small number of library members (0.1%) were highly active. From these we identified 14 potent, gain-of-function, pore-forming sequences. These sequences differed from melittin in only 2−6 amino acids out of 26. Some native residues were highly conserved and others were consistently changed. The two factors that were essential for gain-of-function were the preservation of melittin's proline-dependent break in the middle of the helix and the improvement and extension the amphipathic nature of the α-helix. In particular the highly cationic carboxyl-terminal sequence of melittin, is consistently changed in the gain-of-function variants to a sequence that it is capable of participating in an extended amphipathic α-helix. The most potent variants reside in a membrane-spanning orientation, in contrast to the parent melittin, which is predominantly surface bound. This structural information, taken together with the high-throughput tools developed for this work, enable the identification, refinement and optimization of pore-forming peptides for many potential applications.

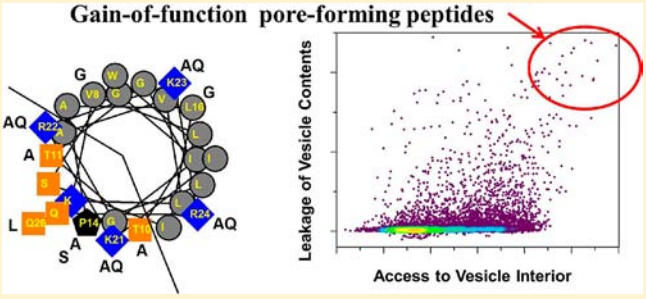

INTRODUCTION

There are many natural and designed peptides that permeabilize membranes, and there are multiple mechanisms by which membrane permeabilization of can occur.[1−3] Yet, peptides that have been shown unequivocally to self-assemble into explicit membrane spanning pores are rare. The design and engineering of such peptide "nanopores" in lipid bilayer membranes is desirable as it could lead to improved biosensor platforms,[4] targeted therapeutics[5−7] or drug delivery vehicles.[8] While the few well studied pore-forming peptides have provided a lot of information about the architecture of peptide pores, especially α-helical pores,[3,9−12] our knowledge of the fundamental molecular principles of pore formation is not detailed enough for outright design or rational engineering. This is a roadblock to the design of new pore-forming peptides and to the optimization of known pores for particular applications.

Because *de novo* design is difficult, researchers often study natural pore-forming peptide toxins instead and try to adapt them to specific functions.[6,13] The natural pore-forming peptide most often used is melittin, the archetypal 26 residue α-helical peptide toxin that is the main component of European Honey Bee venom. Like other helical peptide pore-formers, melittin folds into an amphipathic α-helix with a nonpolar surface that drives partitioning into lipid bilayer membranes.[11,14−16] Its cationic C-terminal segment drives binding to anionic lipids,[17,18] but is probably not α-helical in membranes.[19,20] Melittin's α-helix is separated into two structurally independent segments by a critical, helix-breaking proline residue at position 14 giving rise to a dynamic, disordered pore state.[18,21,22] But, beyond these basic architectural principles, we do not have a detailed, molecular understanding of the mechanism of pore-formation by melittin. One reason for the lack of a detailed understanding of melittin's pore is that its activity is strongly dependent on the details of the system used to study it.[3,9,15,23−27] The "pore" can thus have a wide range of measurable properties, depending on factors such as peptide concentration, lipid composition, pH, ionic strength, and temperature. Another reason why the pore structure of melittin is difficult to define is that the transmembrane pore state is usually a minor component of the total peptide population. In hydrated membranes, melittin is mostly monomeric and mostly has its helical axis predominantly oriented parallel to the membrane surface.[10,23,27] Only a small fraction of peptide is in a pore-competent, transmembrane state at any moment in time.

Received: May 9, 2012
Published: June 25, 2012

   dx.doi.org/10.1021/ja3042004 | J. Am. Chem. Soc. 2012, 134, 12732−12741

Therefore, despite the fact that the general architectural principles of pore formation by helical peptides have been well understood for a long time, we do not yet have a detailed understanding of how the sequence of melittin, or any other pore-former, drives it to self-assemble into transmembrane pores. It is thus difficult to design novel pore-forming sequences or to engineer known sequences, such as melittin, to optimize them for a specific application.

To maximize the potential utility of pore-forming peptides it is necessary to be able to optimize their properties, including their potency as pore-formers. For melittin, an increase in potency could be accomplished by increasing the conductance of the individual peptide pores, or by increasing the steady-state fraction of peptide that is the transmembrane pore state. Attempts to stabilize the transmembrane pore-state of melittin have been made using template-assembled multimers[28−30] which were partially successful. However, this approach involves the synthesis and purification of large, complex macromolecules, which limits its utility. In the work presented here, we take a high-throughput approach to find linear sequence variants of melittin with optimized pore-forming activity. Specially, we used a novel, orthogonal high-throughput assay to select for peptides that assemble into highly potent, *equilibrium* pores in synthetic lipid vesicles.[31] We selected for the most active *gain-of-function* sequence variants from a rational combinatorial peptide library based on melittin in which we allowed ten critical residues to vary. Screening was done at high stringency where melittin's activity is low, thus enabling us to select for variants with higher pore-forming activity than the parent sequence of melittin. The gain-of-function peptides that we identified reveal the sequence features that are essential for optimal efficiency of pore formation in melittin-like peptides. This information will be very useful for *de novo* design and rational redesign of pore-forming peptides. Furthermore, the high-throughput methods developed for this work enable the functional selection of novel pore-forming peptide activities, even when the structural principles of the pore are not well understood.

MATERIALS AND METHODS

Combinatorial Peptide Library Synthesis. The combinatorial peptide library was synthesized on Tentagel NH_2 macrobeads with 50−60 mesh pore size (~50 000 beads per gram) as described in detail elsewhere.[32−35] The quality of the library synthesis was verified by HPLC, mass spectrometry and Edman sequencing of multiple individual beads which revealed correct, full-length sequences. The photocleavable linker attaching the peptide to the bead was cleaved with 5 h of low-power UV light on dry beads spread to a sparse single layer in a glass dish. The beads released an average of 0.5 nmol per bead, which is about one-third of the total peptide on the bead. Histograms of peptide released per bead are Gaussian with mean of ~0.5 nmol and a standard deviation of 0.25 nmol.

When Edman sequencing was performed, it was done directly using the peptide remaining covalently attached to the beads. Even after cleavage of the photolinker and extraction of the free peptides, each bead still had as much as 1 nmol of peptide attached to it, which is several orders of magnitude higher than the minimum sensitivity of Edman sequencing.

The Two-Step Assay. Unilamellar vesicles of 0.1 μm diameter containing 1% NBD-labeled phospholipids were made by extrusion. The vesicles also contained entrapped terbium and external dipicolinic acid for measurement of leakage.[31] In high-throughput screens using the two-step assay, peptide was always present at about 1 μM and lipid concentration was adjusted to achieve P:L = 1:1000. Wells with only liposomes were used as negative controls, and wells with liposomes plus 0.1% (final concentration) reduced Triton-X 100 detergent were used as positive controls. In most samples peptide-induced leakage occurs within 30 min; however we wanted to measure NBD quenching at equilibrium so samples were incubated for at least 8 h. Terbium leakage was then measured, followed by NBD-quenching with dithionite.[31] Using a Biotek Synergy plate reader, DPA-terbium fluorescence was measured with excitation at 284 nm from a xenon flash lamp, and emission at 530 nm. Sensitivity was adjusted so that the detergent-lysed positive controls' arbitrary fluorescence was roughly 30% of the instrument maximum. To assess the accessibility to the interior of the vesicles at equilibrium in the same 96-well plate samples, we measured the quenching of NBD fluorescence as a function of time using band-pass filters of 485/20 (center/width) for excitation and 530/25 for emission. NBD fluorescence was monitored following the addition of 25 μM dithionite from a freshly prepared concentrated stock solution of 0.6 M in pH 10 buffer.[31]

For high-throughput screens, library beads with dry cleaved photolinker were placed into the wells of a polystyrene-V bottom 96-well microplate. Fifty microliters of hexafluoroisopropanol was added to each well and the plate was heated at 80 °C for 10−15 min in a fume hood to extract the peptide from the bead. After complete evaporation of solvent, 100 μL of water with 0.2% sodium azide was added to the wells, and the plate was allowed to incubate for at least 4 h to allow for precipitation of insoluble peptides. Forty microliters from each well was pipetted into a separate plate of containing ~1 mM lipid vesicles with entrapped Tb^{3+} and external dipicolinic acid (DPA) in buffer. The final peptide to lipid ratio (P:L) was ~1:1,000. In parallel, 40 μL of peptide from the initial well was used in a high-throughput screen at P:L = 1:20 for *loss of function* sequences.

ANTS/DPX Leakage. ANTS at 5 mM and DPX at 12.5 mM were entrapped in 0.1 μm diameter extruded vesicles with various lipid compositions as described elsewhere.[36] Leakage was quantitated by the increase in ANTS fluorescence that occurs when the entrapped DPX quencher is diluted into the external buffer upon permeabilization. We prepared ANTS/DPX containing vesicles[36] which were diluted to 1 mM total lipid concentration. Peptide was added at concentrations between 0.5 and 20 μM, giving P:L between 0.0005 (1:2000) and 0.02 (1:50). Leakage was measured after 3 h incubation. The concentration dependence of leakage was fit with a hyperbolic/sigmoidal curve, and the peptide concentration that causes 50% leakage (LIC_{50}) was determined from the curve fits.

Oriented Circular Dichroism. Oriented circular dichroism was performed as described elsewhere.[37] Briefly, lipids and peptide in methanol at P:L = 1:200 were dried into a thin film on a quartz disk which was sealed in a water tight sample holder with a second quartz window. The sample was hydrated to near 100% relative humidity through the vapor phase with a drop of water in the chamber (not touching the sample). Hydration-dependent changes in spectra occurred for about 15 min after sealing the sample holder. All samples were allowed to hydrate for at least 1 h before data was collected. The apparatus was aligned with the beam and 4 spectra were collected with 90° axial rotations of the sample holder between each.

RESULTS

The Two-Step Assay for Equilibrium Pores in Lipid Vesicles. In Figure 1 we show a schematic diagram of the orthogonal two-step assay designed to assess the potency of peptide pores in lipid vesicles (step one), and to independently verify the continued existence of the pores at equilibrium (step two). The latter step of the assay is critical because there are many nonspecific, membrane-destabilizing peptides, including most of the natural host-defense antimicrobial peptides,[38,39] which permeabilize membranes only transiently (i.e., only immediately after addition).[34,40] Peptides that form pores at very low peptide concentration, and which are still present at equilibrium, are rare. We note here that the two-step assay does not distinguish between long-lifetime and short-lifetime pores. It assesses only whether or not pores of any lifetime exist in the

dx.doi.org/10.1021/ja3042004 | J. Am. Chem. Soc. 2012, 134, 12732−12741

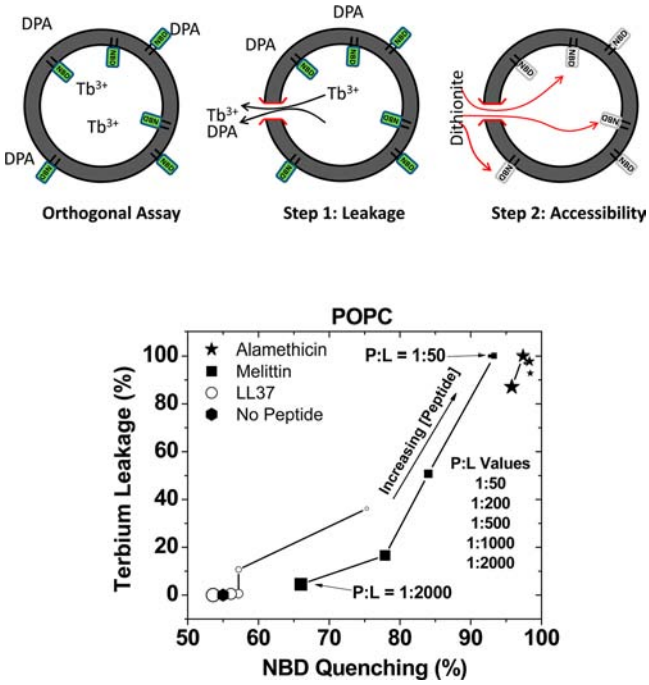

Figure 1. The two-step assay. (Top) Schematic diagram of the components of the two-step assay. Unilamellar lipid vesicles are prepared with entrapped terbium and external dipicolinic acid (DPA) to probe leakage by measurement of complex formation (step one: leakage). In the same vesicles, access of the membrane impermeant quencher dithionite to the vesicle interior at equilibrium is measured by its ability to quench NBD dye-labeled lipids (step two: accessibility). Accessibility to the vesicle interior requires an equilibrium pore in the membrane. (Bottom) Two-step assay measurements of membrane permeabilizing peptides in 100% zwitterionic 1-palmitoyl-2-oleoyl-*sn*-glycero-3-phosphocholine (POPC) vesicles. Symbol sizes reflect total peptide concentration.

membrane at equilibrium (i.e., a few hours after peptide addition). For the assay, unilamellar lipid vesicles are prepared with entrapped terbium and external dipicolinic acid (DPA) to measure permeabilization as we have described elsewhere.[34,35,41,42] In the same vesicles we include a trace of phospholipid labeled on the headgroup with the dye NBD (Figure 1) which can be irreversibly quenched by the membrane impermeant reducing agent dithionite.[43] Quenching of NBD-lipids is done at equilibration, which we define for this work as at least a few hours after addition of peptide. In all experiments the external NBD lipids (~55% of the total) are quenched. At equilibrium, access of the quencher to the vesicles' interior lipid monolayers, which contain the remaining 45% of the NBD-lipid, can only occur if there are active pores in the membranes. In Figure 1 we show two-step assay measurements of leakage and NBD quenching for melittin and two other pore-forming peptides: alamethicin, a potent α-helical pore-former[12] and LL37, a helical cationic antimicrobial peptide that does not form explicit pores in membranes at equilibrium.[31] We used vesicles made from pure zwitterionic phosphatidylcholine (PC) lipids. Data are shown for peptide to lipid ratios, P:L, from 0.0005 (1:2000) to 0.02 (1:50). The 0.1 μm unilamellar lipid vesicles used in this work have about 100,000 lipids each, so the peptide:vesicle ratio ranges from P:V = 2000:1 (for P:L = 1:50) to P:V = 50:1 (for P:L = 1:2000). Under the conditions of these measurements, alamethicin is very potent and form pores at equilibrium at all concentrations studied, as shown by leakage and NBD quenching both near 100% for all P:L values. For comparison, LL37, like all other cationic antimicrobial peptides we have tested,[31] causes leakage only at the highest P:L values, and causes essentially no equilibrium access to the vesicle interior pores at any concentration.

Importantly for this work, the activity of melittin is intermediate. Melittin is a highly active, equilibrium pore-forming peptide at P:L > 0.005 (1:200) but it decreases in activity as P:L is decreased. At P:L = 0.0005 (1 peptide:2000 lipids), melittin's activity is very low. In the work presented here we are using high-throughput screening to identify gain-of-function analogues of melittin that have potent pore-forming activity at P:L ratios where melittin has low activity.

Design of the Melittin Library. The sequence of melittin is shown in Figure 2 along with an α-helical wheel projection.

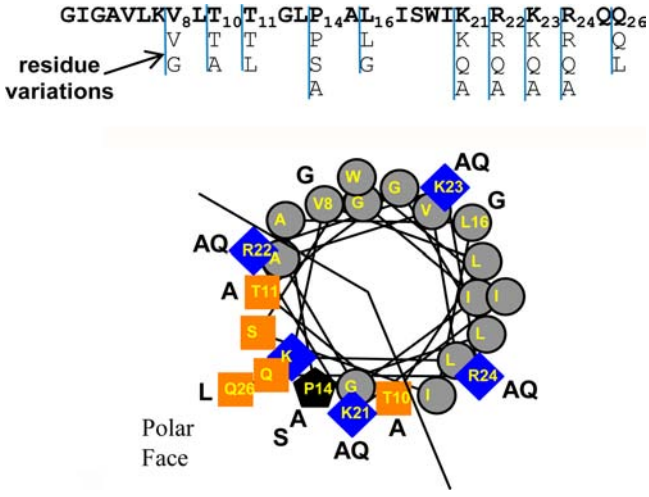

Figure 2. (Top) Amino acid sequence of the pore-forming peptide melittin. Residues that were varied in the combinatorial library are shown. (Bottom) Helical wheel projection of melittin showing the nonpolar and polar faces of the helix. All residues are drawn in helical configuration. Orange symbols represent polar, uncharged residues. Blue symbols represent basic residues. Gray symbols represent hydrophobic residues. The extra one-letter residue codes shown on the helical wheel are the residues that were present in the combinatorial library. Each varied position also always including the native residue.

The surface of the melittin helix can be divided into nonpolar and polar faces as shown. This amphiphilicity drives coupled binding and secondary structure formation.[10] We have drawn the cationic C-terminal tail (..KRKRQQ) in a hypothetical helical conformation, which violates the amphipathicity of the helix by placing K23 on the nonpolar face. While the C-terminal tail sequence is probably not helical under most experimental conditions[19,20] we have drawn it in helical configuration to show that the library contains many members in which the C-terminal tail can participate in an extended amphipathic α-helix. For example, 33% of library members contain the K23A variant.

The library design is shown in Figure 2 where combinatorially varied residues in the melittin sequence are shown. Instead of designing a very large, exhaustive library, we chose 10 residues out of 26 to vary combinatorially so that we could test specific hypotheses about melittin's mechanism of action and the structure of the pore. We used only two or three

dx.doi.org/10.1021/ja3042004 | J. Am. Chem. Soc. 2012, 134, 12732–12741

possible amino acids at each position, always including the native residue. There were five categories of residues that were varied in the library. First, we allowed the C-terminal glutamine to be replaced with leucine to increase hydrophobicity of the very polar C-terminus. Second, we varied the four cationic residues in the C-terminal tail, allowing them to be either a polar, uncharged glutamine or a nonpolar, helix-promoting alanine in addition to the native arginine or lysine. This allows for peptides with reduced C-terminal positive charge, and for peptides with extended helicity and improved amphipathicity. Third, we allowed for the substitution of T10 with alanine and T11 with leucine to change amphipathicity and helix propensity. Alanine and leucine are more hydrophobic than threonine[44] and have much higher helical propensity.[45] A nonpolar amino acid substitution at T10 would also decrease the polar face angle, which is a critical parameter for determining the behavior of amphipathic helices in membranes.[46] Fourth, we allowed for the substitution of glycine at the hydrophobic residues V8 and L16. Together with the glycine at position 12, glycines at position 8 and/or 16 would allow for lateral self-associating opportunities through "glycine zipper" of GXXXG motifs noted in a number of dimeric and oligomeric α-helical transmembrane proteins and channels.[47,48] Fifth, we allowed the critical proline 14 residue to be either alanine or serine in addition to the native proline. While it is known that altering P14 decreases melittin's potency substantially,[49,50] a library-based high-throughput approach allows us to detect synergistic, nonadditive contributions from different residues. Furthermore A14 or S14 sequences provide the opportunity for linear helical peptides in the library that lack the helix disrupting effect of proline.

High-Throughput Screening for Gain-of-Function Analogues of Melittin. The rational combinatorial library in Figure 2 contains 7776 members and was synthesized as a split and recombine (one bead-one sequence) library as we have described in detail elsewhere.[32−35,41] Validation of the library synthesis was done by verifying full-length, single sequences on multiple individual beads by HPLC, sequencing, and mass spectrometry. Beads released ~0.5 ± 0.25 nmol of one peptide sequence each (mean ± standard deviation). The library was screened for high activity and equilibrium pores using the two-step assay (Figure 1) which measures leakage and access to the vesicle interior through a peptide pore at equilibration. Screening was done at a nominal P:L = 0.001 (1:1000), where melittin has low activity (Figure 1), to select for gain-of-function variants of the native sequence. The library was screened by first placing one photocleaved bead in each well of a 96-well plate, extracting the peptide from the bead into buffer, and allowing insoluble library members to precipitate. Then, a portion of the extracted peptide was added to a different 96-well plate containing liposomes to achieve P:L = 1:1000. After equilibration, Tb^{3+} leakage and NBD quenching were assayed by the two-step assay.[31] The results of the whole screen are shown in Figure 3. In panel A, we show a cumulative scatter plot of the leakage and NBD quenching for all 10 000 library members assayed in the high-throughput screen. In panel B we show histograms of the two orthogonal measurements. Notice that at P:L = 1:1000 most library members (>99%) are inactive with leakage near zero. Because we showed that all beads released a similar amount of peptide the distribution of leakage in Figure 3B is mostly a histogram of library member activity. The NBD quenching histogram is bimodal. After equilibration, most samples have NBD

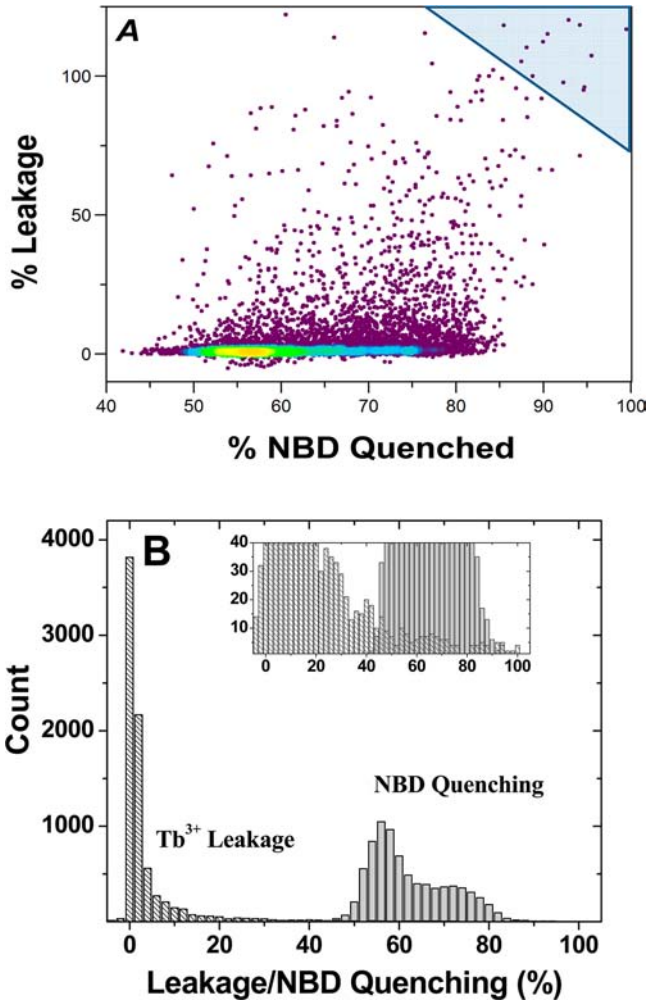

Figure 3. High-throughput screen results. (A) Two-step assay results for all 10 000 library members assayed. The screen was done at a nominal peptide:lipid ratio of 1:1000. Leakage and access of dithionite to NBD-lipids at equilibrium are plotted for each library member assayed. Under these conditions almost all library members are inactive with leakage near 0% and NBD quenching near 55%, indicating only surface exposed lipids are quenched. The area in the triangle at the upper right represents the most active peptides in the library with leakage and NBD-quenching at equilibrium near 100%. (B) Histograms of the data plotted in panel A show that most library members are inactive under these conditions.

quenching around 55%, indicating that there is no peptide-dependent access of the quencher to the vesicle interior. A second broad peak in NBD quenching (from 60 to 80%) suggests that some library members may perturb the bilayer enough to allow NBD lipids to translocate to the exterior monolayer or enough to allow some dithionite inside the vesicles. However almost all of the peptides that cause 60−80% NBD quenching allow no leakage of Tb^{3+}/DPA (Figure 3A) thus we conclude that these peptides are not forming explicit pores in the membrane. In this work we focus only on the peptides that form potent equilibrium pores.

After screening 10 000 peptides, we found that about 0.1% were exceptionally active pore-forming peptides, with Tb^{3+} leakage greater than ~90% and NBD quenching greater than ~85%, indicative of a very potent pore that remains active at equilibrium. This area of the cumulative plot (Figure 3A) is shown by the shaded triangular area (upper right). The

dx.doi.org/10.1021/ja3042004 | J. Am. Chem. Soc. 2012, 134, 12732−12741

G	I	G	A	V	L	K	V	L	T	T	G	L	P	A	L	I	S	W	I	K	R	K	R	Q	Q	Native Sequence	
1	2	3	4	5	6	7	8	9	10	11	12	13	14	15	16	17	18	19	20	21	22	23	24	25	26	Residue #	
Residues present in library							V G		T A	T L			P S A		L G					K A Q	R A Q	K A Q	R A Q		Q L	Two step screen values	
Screening Results																										Tb^{3+}	NBD
G	I	G	A	V	L	K	V	L	A	T	G	L	P	A	L	I	S	W	I	K	R	A	Q	Q	L	105	87
G	I	G	A	V	L	K	V	L	A	T	G	L	P	A	L	I	S	W	I	Q	A	A	Q	Q	L	96	94
G	I	G	A	V	L	K	G	L	A	T	G	L	P	A	L	I	S	W	I	K	Q	A	Q	Q	Q	93	89
G	I	G	A	V	L	K	G	L	T	T	G	L	P	A	L	I	S	W	I	K	A	A	R	Q	L	100	94
G	I	G	A	V	L	K	V	L	A	T	G	L	P	A	L	I	S	W	I	K	A	A	Q	Q	L	92	90
G	I	G	A	V	L	K	V	L	A	T	G	L	P	A	L	I	S	W	I	Q	R	A	R	Q	Q	107	95
G	I	G	A	V	L	K	V	L	A	T	G	L	P	A	L	I	S	W	I	Q	Q	A	Q	Q	L	100	99
G	I	G	A	V	L	K	G	L	A	T	G	L	P	A	L	I	S	W	I	Q	R	A	Q	Q	Q	98	92
G	I	G	A	V	L	K	V	L	T	T	G	L	P	A	L	I	S	W	I	K	Q	A	R	Q	Q	102	84
G	I	G	A	V	L	K	V	L	T	T	G	L	P	A	L	I	S	W	I	K	R	A	Q	Q	Q	100	90
G	I	G	A	V	L	K	V	L	A	T	G	L	P	A	L	I	S	W	I	Q	R	K	Q	Q	Q	96	87
G	I	G	A	V	L	K	V	L	A	T	G	L	P	A	G	I	S	W	I	Q	R	A	R	Q	L	92	83
G	I	G	A	V	L	K	V	L	A	T	G	L	P	A	L	I	S	W	I	Q	R Q	X	R	Q	Q	95	83
G	I	G	A	V	L	K	V	L	A	T	G	L	P	A	L	I	S	W	I	Q	A	Q	Q	Q	L	100	93
Strongly Excluded										L			S A		G					A		K Q	A				

Figure 4. Sequences of 14 gain-of-function analogues identified in the high-throughput screen. The sequence of melittin and the variants present in the library are shown at the top. The screening results are shown at the bottom. The color code is green for conserved residues, blue for changed residues. Those that were excluded from the active variants are shown at the bottom.

Peptide	Sequence	Δ	+
Melittin	G I G A V L K V L T T G L P A L I S W I K R K R Q Q	0	6
Mel-P1	G I G A V L K V L A T G L P A L I S W I K R K R Q Q	1	6
Mel-P2	G I G A V L K V L T T G L P A L I S W I K R A R Q Q	1	5
Mel-P3	G I G A V L K V L A T G L P A L I S W I K R A R Q Q	2	5
Mel-P4	G I G A V L K V L A T G L P A L I S W I Q A A Q Q L	6	2
Mel-P5	G I G A V L K V L A T G L P A L I S W I K A A Q Q L	5	3
Mel-P6	G I G A V L K V L A T G L P A L I S W I K R A Q Q L	4	4
Mel-P7	G I G A V L K V L T T G L P A L I S W I K R A Q Q Q	2	4
Mel-P8	G I G A V L K G L A T G L P A L I S W I Q R A Q Q Q	4	3
Mel-P9	G I G A V L K G L T T G L P A L I S W I K A A Q Q L	4	3

Figure 5. Sequences of the peptides synthesized for further study. Residues shaded red are changed from the parent sequence of melittin. Residues in blue are the basic amino acids in the sequence. Mel-P1 and Mel-P2 are engineered single site variants to test the effect of the commonly observed T10A and K23A substitutions. Mel-P3 is the T10A, K23A double variant. Peptides Mel-P4 through Mel-P9 were actually observed in the screen. Mel-P4, 5, and 6 have T10A and K23A and different numbers of changed residues in the C-terminal tail. Mel-P7, 8, and 9 have other changes observed in the selection, such as V8G or lack the T10A substitution. "Δ" is the number of amino acid changes overall. "+" is the total charge of the peptide.

dx.doi.org/10.1021/ja3042004 | J. Am. Chem. Soc. 2012, 134, 12732−12741

sequences of the active peptides were determined by Edman sequencing of the peptide that remains attached to the bead.

Negative Peptides. At the same time that we screened the melittin library for *gain-of-function* peptides under stringent conditions (P:L 1:1000) we also performed a parallel assay for *loss-of-function* at P:L = 1:20 by measuring leakage and NBD quenching at low lipid concentration. Results are shown in Supporting Information. At this high P:L ratio, melittin and many library members cause ~100% leakage and 100% NBD quenching. But surprisingly, more than 20% of the library members have low activity (leakage <30% and NBD quenching <65%). This is despite the fact that library members are about 75% identical to melittin, on average, and that essentially all beads release the same amount of peptide. Some of the negatives could be insoluble, but it is very unlikely that all of the inactive peptides are insoluble. This observation verifies what we learned from the high stringency screen at P:L = 1:1000: the membrane permeabilizing activity of melittin is sensitive to small changes in sequence.

Conserved Amino Acid Changes in Active Variants. Fourteen of the highly active, equilibrium pore-formers identified in the gain-of-function screen were sequenced (Figure 4). The selected sequences differ from melittin in 2–6 positions out of the 10 that were varied in the library. Some highly conserved features are found in these very active melittin analogues. The native T11, P14, and L16 residues are almost completely conserved among the active sequences ($p < 0.01$). On the other hand, T10 is frequently replaced with alanine. In the residues of the cationic C-terminal tail there are conserved changes. For example, K23 is almost completely replaced by alanine ($P < 0.01$), while alanine is excluded from the K21 and R24 positions ($p < 0.01$) which otherwise have no preference for the original basic residue over a glutamine (Q) ($p > 0.05$). At R22 there is no preference for any of the three possible residues, including the native Arg. At Q26 there is no preference for the native glutamine or the possible leucine. Overall, in the gain-of-function analogues the charge of the C-terminal tail is reduced from +4 in melittin to an average of +1.1 (range 0 to 2; most abundant = +2) in the selected variants.

To validate the screening results and to characterize the melittin variants, we synthesized the nine peptides shown in Figure 5. To test the effects of the commonly observed T10 to A and K23 to A substitutions, we synthesized single residue variants Mel-P1(T10A) and Mel-P2(K23A) and the double Mel-P3 (T10A/K23A). The other six peptides synthesized were directly observed in the screen. Mel-P4, Mel-P5, and Mel-P6 are consensus peptides representing typical gain-of-function sequences observed. They have the common T10A and K23A substitution along with other changes in the C-terminal tail, but otherwise have the native V8, T11, P14 and L16 residues of melittin. The C-terminal charge of these three peptides ranges from zero (Mel-P4) to +2 (Mel-P6) compared to melittin's C-terminal charge of +4. The peptides Mel-P7, Mel-P8, and Mel-P9 were made to explore the effect of less frequently observed variations in residues V8 and T10 in addition to the typical changes in the sequence of the C-terminal tail.

Activity of Gain-of-Function Variants. To validate the high-throughput screening results, we used Tb^{3+}/DPA vesicles to measure the leakage activity of the peptides under conditions that were very similar to the screening conditions. Large unilamellar vesicles made from 100% PC (as in the screen) and vesicles containing 10% anionic PG lipids were tested using purified peptides. The results are similar between them. Leakage as a function of peptide concentration is either sigmoidal or hyperbolic (see Supporting Information for examples), and thus we express potency by measuring the leakage inducing concentration that gives 50% leakage (LIC_{50}) from 1 mM vesicles. All of the selected peptides have higher pore-forming activity (lower LIC_{50}) than melittin in the leakage assay (Figure 6). This result validates the high-throughput

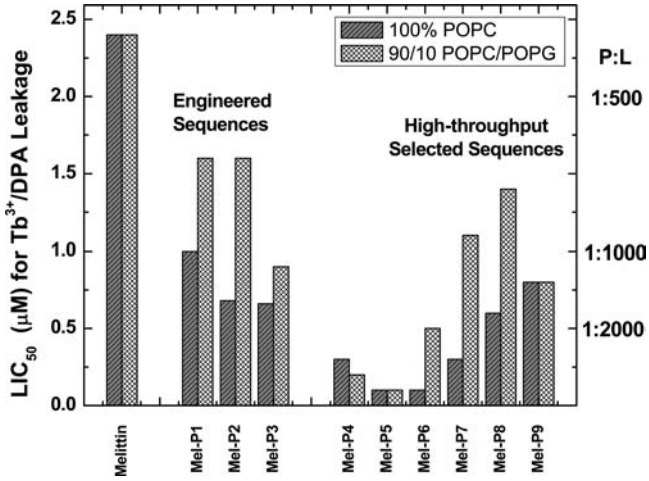

Figure 6. Verification of membrane permeabilization by selected and engineered peptides. Leakage of Tb^{3+}/DPA was measured under conditions very similar to the high-throughput screen. In this experiment we used vesicles made from POPC and 10% POPG (as in the screen). Leakage from 1 mM vesicles was measured as a function of peptide concentration, and the peptide concentration that induces 50% leakage (LIC_{50} or Leakage Inducing Concentration for 50%) was obtained by curve fitting. The engineered sequences differ from the parent by one or two commonly observed substitutions. The selected sequences were actually observed in the high-throughput screen.

screen approach toward gain-of-function. Even the single site variants, Mel-P1 (T10A) and Mel-P2 (K23A) are more active than melittin. The most active of the melittin variants, Mel-P4 and Mel-P5 caused essentially 100% leakage at all concentrations tested, indicating that they form very potent, equilibrium pores under conditions where melittin's activity is very low.

To test the robustness and generality of the observed gain-of-function, we also measured the membrane permeabilizing activity of melittin and the variants in a variety of lipid compositions, using a different leakage indicator system in a different buffer. Measurements such as these are necessary to show that we did not select for activity that was highly dependent on the details of the high-throughput screening system. Also, in these experiments, we measured leakage after only 1 h to eliminate the effect of slow processes we might have selected for in the (overnight) high-throughput screens. Vesicles of five different lipid compositions, containing the entrapped fluorophore ANTS and its obligate quencher DPX, were used to mimic the range of compositions that occur naturally in biomembranes. The buffer in the ANTS/DPX leakage was 10 mM phosphate with 40 mM NaCl, pH 7.0, in comparison to the 10 mM TES, 300 mM NaCl, pH 7.2 buffer used in the Tb^{3+}/DPA assay. Despite the significant differences in ionic strength, leakage probe, and incubation time, the results in Figure 7 show that the gain-of-function variants have

dx.doi.org/10.1021/ja3042004 | J. Am. Chem. Soc. 2012, 134, 12732–12741

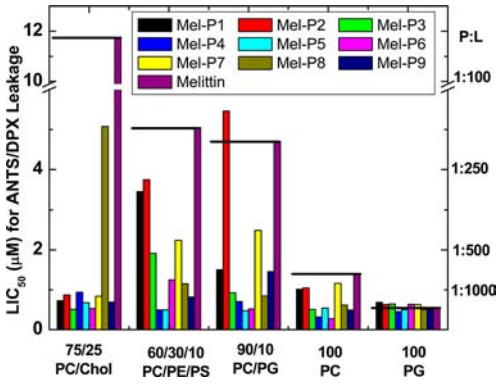

Figure 7. Membrane permeabilization by selected and engineered peptides. Leakage of ANTS/DPX was measured by fluorescence. In this experiment we used vesicles made from various lipid compositions. Leakage from 1 mM vesicles was measured as a function of peptide concentration, and the peptide concentration that induces 50% leakage (LIC50 or Leakage Inducing Concentration for 50%) was obtained by curve fitting.

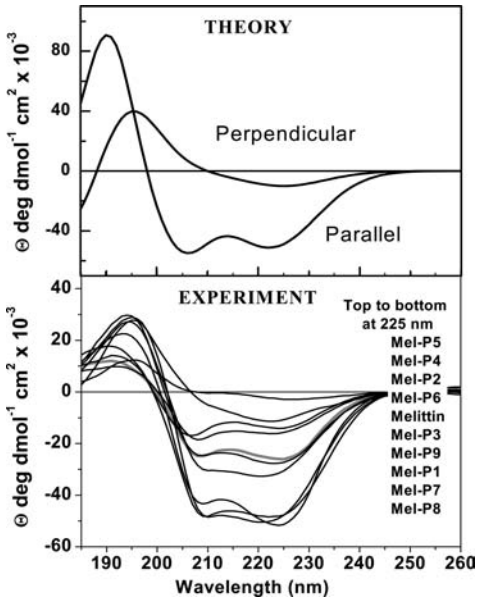

Figure 8. Oriented circular dichroism. (Top) Theoretical oriented CD spectra for 100% inserted (perpendicular) and 100% surface bound (parallel) α-helical peptides.[53] (Bottom) Melittin or one of the nine gain-of-function analogues were incorporated into stacked oriented multibilayers deposited on a quartz disk. Samples were enclosed in a chamber with a drop of water for hydration through the vapor phase and oriented CD spectra were taken. The lipid used was pure POPC and the P:L ratio was 1:200 for all samples.

consistently higher activity than melittin in all lipid compositions, except for pure PG vesicles. This verifies the generality of the gain-of-function. The "consensus" sequences Mel-P4, Mel-P5, and Mel-P6 are consistently 5−20 fold more potent than melittin. Interestingly, the presence of cholesterol reduces melittin's activity dramatically while having a much smaller effect on the activity of the gain-of-function variants. In bilayers composed of pure anionic PG lipids, melittin itself is especially active and thus the difference between melittin and the variants is smaller.

Membrane Orientation of the Gain-of-Function Variants. Melittin and the gain-of-function variants bind similarly to PC membranes and to membranes containing 10 mol % PG lipids (see Supporting Information). When bound to lipid vesicles, all of the peptides including melittin have similar amounts α-helical secondary structure. This means that the differences in pore-forming activity are probably due to more subtle changes in pore structure, or in the steady-state fraction of peptide residing in the transmembrane pore state. Because the membrane-spanning pore state of melittin is only a minor fraction of the total peptide,[3,23,25,51] we tested the hypothesis that the gain-of-function variants have a larger steady state fraction of membrane-spanning peptide. To assess whether the peptides are mostly surface bound (parallel to the membrane surface) or are mostly perpendicular transmembrane), we performed oriented circular dichroism (OCD) on oriented multibilayer samples as described elsewhere.[52,53] The OCD spectra for the theoretical parallel and perpendicular orientations are very distinct.[53] A transmembrane helix has a small minimum in ellipticity at 230 nm and a maximum at 195−200 nm, whereas a surface bound helix gives two large minima at 208 and 225 nm and maximum at 190−195 nm (Figure 8). Mixtures of orientations or insertion angles between 0 and 90° angles give OCD spectra intermediate between the two theoretical spectra shown in Figure 8 (above). All of the OCD experiments in Figure 8 were performed at identical peptide and lipid concentrations, with P:L = 1:200 so they are directly comparable to one another. The oriented CD spectrum of melittin is consistent with the conclusion of others[23,27] that it is mainly parallel to the bilayer surface (not inserted) at equilibrium. This is shown by the two large minima in its OCD spectra at 208 and 225 nm. By the same criterion, many of the melittin variants are also mostly parallel to the bilayer surface (<30% inserted). However, a subset of the variants (the consensus sequences Mel-P4, -P5, and -P6) have a higher fraction inserted into the membrane as a transmembrane helix under these conditions. Specifically, Mel-P4 and Mel-P5, which are the most potent pore-formers in the group (Figures 6 and 7) are almost completely inserted (>80%) inserted into a transmembrane orientation in the membrane at equilibrium.

DISCUSSION

Gain-of-Function Variants of a Pore-Forming Peptide. For this work we define a *potent*, pore-forming peptide as one that permeabilizes synthetic lipid vesicles at low peptide:lipid ratio (P:L ≤ 1:1000). We define an *equilibrium* pore as one that remains detectable in bilayers after equilibration for 1 h or more. We are not assuming that an equilibrium pore is necessarily a stable or long-lived structure. It could also be one that forms and dissipates continuously. Importantly this definition excludes the well-known (and very abundant) cationic antimicrobial peptides (e.g., cecropins, magainins, defensins, cathelicidins). Instead of forming potent, equilibrium pores, they act by interfacial activity[1,42] against synthetic and biological membranes. Antimicrobial peptides typically permeabilize lipid vesicles only at high concentration (P:L ≥ 1:100) and form transient pores that are typically not present at equilibrium.[31] While there are more than 1000 cationic antimicrobial peptides described in the literature,[54] there are no more than a few dozen potent, equilibrium pore-forming peptides known. Only a small number of these have been studied in detail, and our knowledge about them is not sufficient for rational design or engineering of activity. Here we showed that the novel two-step assay can be used in a high-throughput format to select for highly active equilibrium pore-

forming peptides even in the absence of detailed structural information about the pore. By applying this new approach to a hypothesis-based, melittin-derived combinatorial library we were able to select gain-of-function variants of melittin that were significantly more active than the parent peptide melittin.

Sequence and Structure of Gain-of-Function Variants of Melittin. The structure of the melittin pore has been studied for decades, yet it has been difficult to describe in explicit molecular terms. In part, this is because the pore is disordered and highly dynamic, and can have a wide range of measurable properties, depending on factors such as peptide concentration, lipid composition, solution pH, ionic strength, and temperature.[3,9,25,26] From in-plane neutron scattering in zwitterionic phosphatidylcholine membranes at low hydration, the melittin pore has been described as a "toroidal pore", in which peptides form a membrane-spanning structure by cooperatively changing the local curvature of the lipid bilayer[55] without specific lateral interactions between peptides. But in fully hydrated bilayers (e.g., Figure 8) melittin is predominantly oriented parallel to the bilayer surface,[10,23,27] and the presumed membrane-spanning pore state is only a minor fraction of the total peptide population. In the absence of a molecular understanding of the pore structure, the approach we used here to identify gain-of-function variants is especially useful because (1) selection is based on observed activity and is not dependent on understanding the mechanism, and (2) rational libraries can be designed to test specific structural hypotheses via high-throughput screening, thus improving our understanding of the mechanism of pore formation.

The library design used here allowed us to test three major factors: (1) the importance of proline kink, (2) the importance of the overall amphipathicity of the helix, and (3) the importance of the highly polar, cationic C-terminal tail. The absolute conservation of P14 we observed is the least surprising observation, as it has been shown previously to be important for melittin's activity.[49,50] This is presumably because the helix-interrupting proline 14 (along with glycine 12) allow for the formation of a kinked structure, creating an hourglass-shaped pore through the membrane.[21] Some other helical pore-forming peptides, such as alamethicin,[12,56] also contain central proline kinks. But there are also potent pore-forming peptides that do not have a proline or glycine kink. We recently compared the proline containing pore-formers melittin and alamethicin with the proline-free pore-forming peptides LLP1 and LLP2[31,57] and found that the proline-containing peptides, melittin and alamethicin, readily exchange between bilayers, while the proline-free LLP peptides do not.[31] This observation supports the conclusion that the proline kink of melittin allows for the formation of a dynamic, disordered pore in the membrane. The complete conservation of the proline residue in this high-throughput screen shows that it is required for potent activity in the context of these melittin-like peptides. The two other highly conserved residues, T11 and L16, are both close to the P14 kink in the melittin α-helix, supporting the idea that the proline break is an important structural feature of melittin-like pore formation.

Most of the changed/conserved residues in the gain-of-function variants indicate that an ideal amphipathic helix is the other critical factor in the gain-of-function. Observations that support this idea are (1) the frequent conservation of V8, T11, and L16, which preserves their polar nonpolar segregation; (2) the exclusion of alanine from K21 and K24, which preserves the polarity of the helical polar face; and (3) the frequent change of the nonpolar face residues T10 and K23 to alanine. Residue K23 may be especially important because it resides in the middle the nonpolar face in the hypothetical extended helix (Figure 2) encompassing the cationic C-terminal tail. The C-terminal tail may not be helical in membranes in the parent sequence of melittin, but our results suggest that the C-terminal tail in the gain-of-function variants is part of an extended amphipathic helix that gives rise to increased activity. This observation agrees with the published observation that substitution of some C-terminal basic residues with leucine increases the hemolytic activity of melittin.[58] It has been shown that the cationic C-terminal tail of melittin drives strong binding to anionic lipids[17,19,20,59] This probably explains why native melittin is especially active against pure PG vesicles (Figure 7). Our observations indicate that the native C-terminal tail does not have a critical functional role in pore formation. In support of this idea, it has been shown that deletion of C-terminal residues has little effect on melittin's activity.[60,61] In fact, our results show that the native C-terminal tail inhibits pore formation in most membranes compared to the optimal sequences selected in the high-throughput screen.

Pore-forming activity was shown in this work to be sensitive to peptide sequence even within our melittin-based library which explores only a narrow region of sequence space. We screened thousands of peptides that are very similar to melittin and the majority have similar activity. Interestingly, about 20% of the library is inactive even at very high P:L ratios. Most importantly for this work, a small fraction of the library members (0.1%) have significantly better activity than the parent sequence of melittin. Even a single residue change can improve pore-forming activity. For example, the single-site variants T10A (Mel-P1) and K23A (Mel-P2) are more potent than the parent melittin in almost all assays. The consensus sequences Mel-P4, -P5, and -P6 are consistently up to 20-fold more active than melittin. Membrane binding and overall α-helical secondary structure content in water and in membranes are similar for melittin and the gain-of-function variants (see Supporting Information) and thus cannot explain the differences in pore-forming activity. Instead, changes in pore properties must be responsible for the overall potency. Here we showed that the increase in activity for some (but not all) of the variants may be explained by a significant increase in the steady-state fraction of peptide that is in a transmembrane state. The two most active consensus variants, Mel-P4 and Mel-P5, which differ from melittin in 5 or 6 residues, are essentially fully transmembrane at equilibrium. We hypothesize that the more ideal amphipathic helix is driving these highly active gain-of-function peptides to adopt a transmembrane configuration. As a result, the most potent gain-of-function variants behave much more like the potent, fully transmembrane pore-former alamethicin[52,62] than the parent sequence melittin. Presumably, the highly populated transmembrane pore state of MelP4 and MelP5 retain the critical structural features of the sparsely populated native melittin pore state. This raises the intriguing possibility that these predominantly transmembrane gain-of-function variants could be used for structural studies of the pore state, which have not been possible before.

■ CONCLUSION

Here we have shown that combinatorial chemistry and high-throughput screening can be used to find potent gain-of-function analogues of a natural pore-forming peptide even in the absence of a detailed molecular understanding of the pore

itself. This is important for the future design and optimization of pore-forming peptides because we cannot engineer them rationally using our current state of knowledge. Furthermore, by screening libraries designed to test structural hypotheses, we can obtain important information about molecular mechanism of pore formation. This information, in turn, can be used to improve the design of iterative libraries. This feedback-based approach to pore-forming peptide activity enables the optimization, refinement, and discovery of pore-forming peptides for many potential applications.

■ ASSOCIATED CONTENT

Supporting Information

Auxiliary data and images supporting the conclusion of this work. This material is available free of charge via the Internet at http://pubs.acs.org.

■ AUTHOR INFORMATION

Corresponding Author

wwimley@tulane.edu

Notes

The authors declare no competing financial interest.

■ ACKNOWLEDGMENTS

The authors thank Christopher M. Bishop for peptide synthesis and purification, Andrew R. Hoffmann for contributing to leakage experiments, and Thomas C. Freeman Jr. for data analysis software. Funded by NIH grant GM060000 and NSF grant DMR-1003411.

■ REFERENCES

(1) Wimley, W. C. *ACS Chem. Biol.* **2010**, *5*, 905−917.
(2) Matsuzaki, K. *Biochim. Biophys. Acta* **1998**, *1376*, 391−400.
(3) van den, B. G.; Guzman, J. V.; Mika, J. T.; Poolman, B. *J. Biol. Chem.* **2008**, *283*, 33854−33857.
(4) Bayley, H.; Jayasinghe, L. *Mol. Membr. Biol.* **2004**, *21*, 209−220.
(5) Jo, M.; Park, M. H.; Kollipara, P. S.; An, B. J.; Song, H. S.; Han, S. B.; Kim, J. H.; Song, M. J.; Hong, J. T. *Toxicol. Appl. Pharmacol.* **2012**, *258*, 72−81.
(6) Soman, N. R.; Baldwin, S. L.; Hu, G.; Marsh, J. N.; Lanza, G. M.; Heuser, J. E.; Arbeit, J. M.; Wickline, S. A.; Schlesinger, P. H. *J. Clin. Invest* **2009**, *119*, 2830−2842.
(7) Holle, L.; Song, W.; Holle, E.; Wei, Y.; Li, J.; Wagner, T. E.; Yu, X. *Int. J. Oncol.* **2009**, *35*, 829−835.
(8) Gerlach, S. L.; Rathinakumar, R.; Chakravarty, G.; Goransson, U.; Wimley, W. C.; Darwin, S. P.; Mondal, D. *Biopolymers* **2010**, *94*, 617−625.
(9) Raghuraman, H.; Chattopadhyay, A. *Biosci. Rep.* **2007**, *27*, 189−223.
(10) Ladokhin, A. S.; White, S. H. *J. Mol. Biol.* **1999**, *285*, 1363−1369.
(11) Bechinger, B. *J. Membr. Biol.* **1997**, *156*, 197−211.
(12) Cafiso, D. S. *Annu. Rev. Biophys. Biomol. Struct.* **1994**, *23*, 141−165.
(13) Jaikaran, D. C. J.; Biggin, P. C.; Wenschuh, H.; Sansom, M. S. P.; Woolley, G. A. *Biochemistry* **1997**, *73*, 13873−13881.
(14) Terwilliger, T. C.; Weisman, L.; Eisenberg, D. *Biophys. J.* **1982**, *37*, 353−361.
(15) Dempsey, C. E. *Biochim. Biophys. Acta* **1990**, *1031*, 143−161.
(16) Klocek, G.; Schulthess, T.; Shai, Y.; Seelig, J. *Biochemistry* **2009**, *48*, 2586−2596.
(17) Hall, K.; Lee, T. H.; Aguilar, M. I. *J. Mol. Recognit.* **2011**, *24*, 108−118.
(18) Beschiaschvili, G.; Seelig, J. *Biochemistry* **1990**, *29*, 52−58.
(19) Okada, A.; Wakamatsu, K.; Miyazawa, T.; Higashijima, T. *Biochemistry* **1994**, *33*, 9438−9446.
(20) Yuan, P.; Fisher, P. J.; Prendergast, F. G.; Kemple, M. D. *Biophys. J.* **1996**, *70*, 2223−2238.
(21) Sengupta, D.; Leontiadou, H.; Mark, A. E.; Marrink, S. J. *Biochim. Biophys. Acta* **2008**, *1778*, 2308−2317.
(22) Huang, H. W.; Chen, F. Y.; Lee, M. T. *Phys. Rev. Lett.* **2004**, *92*, 198304.
(23) Hristova, K.; Dempsey, C. E.; White, S. H. *Biophys. J.* **2001**, *80*, 801−811.
(24) Dempsey, C. E.; Butler, G. S. *Biochemistry* **1992**, *31*, 11973−11977.
(25) Ladokhin, A. S.; White, S. H. *Biochim. Biophys. Acta* **2001**, *1514*, 253−260.
(26) Pott, T.; Paternostre, M.; Dufourc, E. J. *Eur. Biophys. J. Biophys. Lett.* **1998**, *27*, 237−245.
(27) Frey, S.; Tamm, L. K. *Biophys. J.* **1991**, *60*, 922−930.
(28) Takei, J.; Rényi, A.; Clarke, A. R.; Dempsey, C. E. *Biochemistry* **1998**, *37*, 5699−5708.
(29) Chaloin, L.; Mery, J.; Van Mau, N.; Divita, G.; Heitz, F. *J. Pept. Sci.* **1999**, *5*, 381−391.
(30) Pawlak, M.; Meseth, U.; Dhanapal, B.; Mutter, M.; Vogel, H. *Protein Sci.* **1994**, *3*, 1788−1805.
(31) Krauson, A. J.; He, J.; Wimley, W. C. *Biochim. Biophys. Acta* **2012**, *1818*, 1625−1632.
(32) Marks, J. R.; Placone, J.; Hristova, K.; Wimley, W. C. *J. Am. Chem. Soc.* **2011**, *133*, 8995−9004.
(33) He, L.; Hoffmann, A. R.; Serrano, C.; Hristova, K.; Wimley, W. C. *J. Mol. Biol.* **2011**, *412*, 43−54.
(34) Rathinakumar, R.; Wimley, W. C. *J. Am. Chem. Soc.* **2008**, *130*, 9849−9858.
(35) Rausch, J. M.; Marks, J. R.; Wimley, W. C. *Proc. Natl. Acad. Sci. U.S.A.* **2005**, *102*, 10511−10515.
(36) Ladokhin, A. S.; Wimley, W. C.; Hristova, K.; White, S. H. *Methods Enzymol.* **1997**, *278*, 474−486.
(37) Wimley, W. C.; White, S. H. *Biochemistry* **2000**, *39*, 4432−4442.
(38) Wimley, W. C.; Hristova, K. *J. Membr. Biol.* **2011**, *239*, 27−34.
(39) Hancock, R. E.; Sahl, H. G. *Nat. Biotechnol.* **2006**, *24*, 1551−1557.
(40) Rausch, J. M.; Marks, J. R.; Rathinakumar, R.; Wimley, W. C. *Biochemistry* **2007**, *46*, 12124−12139.
(41) Rathinakumar, R.; Wimley, W. C. *FASEB J.* **2010**, *24*, 3232−3238.
(42) Rathinakumar, R.; Walkenhorst, W. F.; Wimley, W. C. *J. Am. Chem. Soc.* **2009**, *131*, 7609−7617.
(43) Moss, R. A.; Bhattacharya, S. *J. Am. Chem. Soc.* **1995**, *117*, 8688−8689.
(44) Wimley, W. C.; White, S. H. *Nat. Struct. Biol.* **1996**, *3*, 842−848.
(45) Baldwin, R. L. *Biophys. Chem.* **1995**, *55*, 127−135.
(46) Segrest, J. P.; Garber, D. W.; Brouillette, C. G.; Harvey, S. C.; Anantharamaiah, G. M. *Adv. Protein Chem.* **1994**, *45*, 303−369.
(47) MacKenzie, K. R.; Prestegard, J. H.; Engelman, D. M. *Science* **1997**, *276*, 131−133.
(48) Brosig, B.; Langosch, D. *Protein Sci.* **1998**, *7*, 1052−1056.
(49) Dempsey, C. E.; Bazzo, R.; Harvey, T. S.; Syperek, I.; Boheim, G.; Campbell, I. D. *FEBS Lett.* **1991**, *281*, 240−244.
(50) Rex, S. *Biophys. Chem.* **2000**, *85*, 209−228.
(51) Raghuraman, H.; Chattopadhyay, A. *Biophys. J.* **2007**, *92*, 1271−1283.
(52) He, K.; Ludtke, S. J.; Heller, W. T.; Huang, H. W. *Biophys. J.* **1996**, *71*, 2669−2679.
(53) Wu, Y.; Huang, H. W.; Olah, G. A. *Biophys. J.* **1990**, *57*, 797−806.
(54) Fjell, C. D.; Hancock, R. E.; Cherkasov, A. *Bioinformatics* **2007**, *23*, 1148−1155.
(55) Yang, L.; Weiss, T. M.; Harroun, T. A.; Heller, W. T.; Huang, H. W. *Biophys. J.* **1999**, *77*, 2648−2656.
(56) Leitgeb, B.; Szekeres, A.; Manczinger, L.; Vagvolgyi, C.; Kredics, L. *Chem. Biodivers.* **2007**, *4*, 1027−1051.

(57) Costin, J. M.; Rausch, J. M.; Garry, R. F.; Wimley, W. C. *Virol. J.* **2007**, *4*, 123.
(58) Blondelle, S. E.; Houghten, R. A. *Pept. Res.* **1991**, *4*, 12−18.
(59) Chatterjee, C.; Mukhopadhyay, C. *Biochem. Biophys. Res. Commun.* **2002**, *292*, 579−585.
(60) Blondelle, S. E.; Houghten, R. A. *Biochemistry* **1991**, *30*, 4671−4678.
(61) Pérez-Payá, E.; Houghten, R. A.; Blondelle, S. E. *Biochem. J.* **1994**, *299*, 587−591.
(62) Qian, S.; Wang, W.; Yang, L.; Huang, H. W. *Biophys. J.* **2008**, *94*, 3512−3522.